Global observables and secondary interactions in central Au+Au reactions at $\sqrt{s} = 200$ AGeV

M.J. Bleicher[aξ*], S.A. Bass[bξ], L.V. Bravina[cd], W. Greiner[e], S. Soff[f],

H. Stöcker[e], N. Xu[a], E.E. Zabrodin[cd]

[a] *Nuclear Science Division, Lawrence Berkeley Laboratory, Berkeley, CA 94720, U.S.A.*

[b] *Department of Physics, Duke University, Durham, N.C. 27708-0305, USA*

[c] *Institut für Theoretische Physik, Universität Tübingen, 72076 Tübingen, Germany*

[d] *Institut for Nuclear Physics, Moscow State University, 119899 Moscow, Russia*

[e] *Institut für Theoretische Physik, Goethe-Universität, 60054 Frankfurt am Main, Germany*

[f] *Gesellschaft für Schwerionenforschung, Darmstadt, Germany*

Abstract

The Ultra-relativistic Quantum Molecular Dynamics model (UrQMD) is used to study global observables in central reactions of Au+Au at $\sqrt{s} = 200$ AGeV (RHIC). Strong stopping governed by massive particle production is predicted if secondary interactions are taken into account. The underlying string dynamics and the early hadronic decoupling implies only small transverse expansion rates. However, rescattering with mesons is found to act as a source of pressure leading to additional flow of baryons and kaons, while cooling down pions.

LBNL-preprint: LBNL-44599

ξ Feodor Lynen Fellow of the Alexander v. Humboldt Foundation

*E-mail: bleicher@nta2.lbl.gov

One of the major goals of the relativistic heavy ion collider (RHIC) at Brookhaven National Laboratory is to explore the phase diagram of hot and dense matter near the quark gluon plasma (QGP) phase transition. The QGP is a state in which the individual hadrons dissolve into a gas of free (or almost free) quarks and gluons in strongly compressed and hot matter (for recent reviews on the topic, we refer to [1,2]). The achievable energy- and baryon densities sensitively depend on the extend to which the nuclei are stopped during penetration; they also depend on mass number and bombarding energy.

Earlier RHIC estimates have been performed assuming boost-invariant hydrodynamics [3–7] and pQCD (Regge theory) motivated model [8,9]: baryons are concentrated at projectile and target rapidity separated by a large region which is baryon free (in position and momentum space), i.e. the nuclei are transparent. The region between them is filled by the color fields which materialize, developing a plateau in the mesons' rapidity distribution. This scenario is supported experimentally for pp- and p$\bar{\text{p}}$-collisions at collider energies. It is the aim of the present work to examine whether this remains true also for the collision of large nuclei. From lower energy nucleus-nucleus collisions we know that only a small fraction of the total number of collisions takes place at the full incident energy while most of them take place at much lower energies. In fact, transport model studies show a fair amount of stopping at the RHIC energy with strong transverse expansion [10,11] indicating that the collision of two nuclei is more than just the superposition of "A×A" nucleon collisions at the same energy (i.e. that secondary interactions are very important at all investigated energies).

As a tool for our investigation of heavy ion reactions at RHIC the Ultra-relativistic Quantum Molecular Dynamics model (UrQMD 1.2) is applied [12].

Similar to the RQMD model [10,13], UrQMD is a microscopic transport approach based on the covariant propagation of constituent quarks and diquarks accompanied by mesonic and baryonic degrees of freedom. It simulates multiple interactions of ingoing and newly produced particles, the excitation and fragmentation of color strings and the formation and decay of hadronic resonances. At RHIC energies, the treatment of subhadronic degrees of

freedom is of major importance. In the UrQMD model, these degrees of freedom enter via the introduction of a formation time for hadrons produced in the fragmentation of strings [14–16]. The leading hadrons of the fragmenting strings contain the valence-quarks of the original excited hadron. In UrQMD they are allowed to interact even during their formation time, with a reduced cross section defined by the additive quark model, thus accounting for the original valence quarks contained in that hadron [12]. Those leading hadrons therefore represent a simplified picture of the leading (di)quarks of the fragmenting string. Newly produced (di)quarks do, in the present model, not interact until they have coalesced into hadrons – however, they contribute to the energy density of the system. A more advanced treatment of the partonic degrees of freedom during the formation time ought to include soft and hard parton scattering [8] and the explicit time-dependence of the color interaction between the expanding quantum wave-packets [17]. However, such an improved treatment of the internal hadron dynamics has not been implemented for light quarks into the present model. For further details about the UrQMD model, the reader is referred to Ref. [12].

The UrQMD model has been applied successfully to explore heavy ion reactions from AGS energies ($E_{lab} = 1 - 10$ AGeV) up to the full CERN-SPS energy ($E_{lab} = 160$ AGeV). This includes detailed studies of thermalization [18], particle abundancies and spectra [19], strangeness production [20], photonic and leptonic probes [21] , J/Ψ's [22] and event-by-event fluctuations [23].

Let us tackle directly the relevant questions prompted by the start-up of RHIC:

- Can string models like UrQMD be applied to AA reactions at RHIC energies?
- Is baryonic stopping achieved at RHIC?
- How many particles will be produced?
- Will secondary interactions modify observables?

The increasing importance of perturbative QCD effects (hard scattering) [8,9,24] and coherent parton dynamics [25] has lead to the speculations that transport models with

string dynamics will fail to describe heavy ion collisions above a certain center of mass energy. Indeed, todays transport models are based on a probabilistic phase space approach, even in the earliest stage of the reaction. In this stage at RHIC energies, the protons and neutrons of the colliding nuclei should be described by coherent parton wave functions and should be modelled as such [25]. However, after initial parton or string production has taken place in the first 0.5 fm/c [26], this coherence is lost and the UrQMD ansatz may be applicable.

To study the pQCD-induced effects it has been suggested to use the Parton Cascade Model (PCM/VNI) [8] to simulate the dynamics of the hot and dense region of heavy ion reactions. However, the interplay of hard vs. soft physics (early stage vs. late stage of the collision) allows use of these models only in the very early stage of the reaction. Recently it was shown that the large amount of non-perturbative parton interactions at SPS and RHIC energies imposes severe limitations to the applicability of such an approach [27,2].

In fact, higher twist phenomena seem to play an important role at RHIC energies, making leading order (and next-to leading order) perturbative QCD (pQCD) calculations questionable for the study of dense matter [27,28]. It has been argued [29,30], that for subsequent ($t > 1$ fm/c) collision stages, the use of phenomenological approaches to investigate the collision dynamics is inevitable, especially when the system becomes relatively dilute and secondary collisions occur at moderate energies.

It is not known a priori at RHIC energies, whether pQCD effects (presumably taking place at the early stage of the collision, $t \sim 1$ fm/c) or the hadronic rescatterings dominate the evolution of the system and the hadronic spectra measured by the experiments after freeze-out. Models like UrQMD [12] or RQMD [13] can help to identify in the observables signals from different (early/late) stages of the collision dynamics.

Let us investigate UrQMD predictions at increasing center of mass energies for light-ion and proton-proton reactions. UrQMD calculations to rapidity distributions for He+He at $\sqrt{s} = 31$ GeV (ISR) yield good agreement between model and data [12]. If the energy is increased further, pp interactions from UrQMD start to deviate from pQCD motivated

extrapolations by 35% at $\sqrt{s} = 200$ GeV. This deviation is consistent with early attempts made in the RQMD approach as discussed in ref. [10]. It can be pinned down to multi-jet events: here the incoming hadrons do fragment not only into two jets (lead by the incoming quarks/diquarks) but also into additional jets stemming from momentum transfer to the sea-partons of the incoming hadrons. These additional jets result in an overall increase of particle production from center of mass energies of $\sqrt{s} = 100$ GeV upwards. Consequently, this model cannot be applied to pQCD dominated observables, e.g. the high-momentum ($p_t > 2$ GeV/c) part of hadronic spectra or multi-jet related quantities. On the other hand, as will be discussed below, only a minor part of all elementary interactions takes place at such high energies, thus final results in terms of particle multiplicity and spectral shape are only moderately affected, on the order of 10% [10].

Figure 1 shows the $\sqrt{s}$-collision spectra of individual hadron (quark) collisions in Au+Au reactions at $\sqrt{s} = 200$ GeV. Fig. 1a indicates all baryon-baryon (BB) and diquark-diquark collisions, Fig.1b shows meson-baryon (MB) and quark-diquark reactions and Fig.1c describes meson-meson (MM) and quark-quark collisions. All spectra are strongly decreasing towards high collision energies. However, the initial baryon-baryon (diquark-diquark) interactions are visible as a bump around the beam energy of $\sqrt{s} = 200$ GeV (the width of this bump is given by the Fermi-momentum multiplied by the Lorentzfactor).

One observes that the total number of collisions is dominated by secondary interactions. The initial high energy collisions ($\sqrt{s} > 100$ GeV) constitute less than 20% of all reactions. The remaining 80% of the reactions are well treatable by string physics and effective constituent quark dynamics. The average collision energies are given by:

$$\langle\sqrt{s}\rangle = \frac{\int \mathrm{d}\sqrt{s}\,\sqrt{s}\,\frac{\mathrm{d}N}{\mathrm{d}\sqrt{s}}}{\int \mathrm{d}\sqrt{s}\,\frac{\mathrm{d}N}{\mathrm{d}\sqrt{s}}} \tag{1}$$

resulting in $\langle\sqrt{s}\rangle^{\mathrm{MM}} = 1.2$ GeV, $\langle\sqrt{s}\rangle^{\mathrm{MB}} = 2.3$ GeV and $\langle\sqrt{s}\rangle^{\mathrm{BB}} = 8.2$ GeV. It is interesting that the BB value is mostly driven by the initial collisions. If only reactions below $\sqrt{s} = 100$ GeV are counted, $\langle\sqrt{s}\rangle^{\mathrm{BB}}_{\sqrt{s}<100\ \mathrm{GeV}} = 4.6$ GeV. Note that these moderate collision energies are also encountered in 'pQCD' based approaches, e.g. VNI [27]. Thus pointing to a strong

non-perturbative component in the parton-hadron dynamics at RHIC energies.

In the following two different scenarios will be explored in order to study the influence of secondary interactions: UrQMD calculations with the full collision term included will be contrasted by UrQMD simulations with deactivated meson-meson and meson-baryon interactions. The following interactions have been deactivated: Meson-meson, meson-baryon, valence quark-meson, diquark-meson, valence quark-valence quark, valence quark-diquark (incl. anti-quarks and baryons). Note that baryon-baryon, diquark-baryon and diquark-diquark collisions are still possible. This is in contrast to first collision models: In the UrQMD model 'without rescattering' not only multiple baryon-baryon interactions are allowed, but also baryon–anti-baryon annihilations are still possible (cf. Tab. I).

Let us investigate the total energy deposition in calorimeters in terms of the transverse energy E_T:

$$E_T = \sum \left(E_i \sin \theta_i + m_i \right) \quad , \quad \theta_i = \arctan \frac{p_{i\perp}}{p_{i||}} \quad . \tag{2}$$

E_i is the energy of particle i, m_i is the restmass of particle i - if it is an anti-baryon, otherwise it is zero. The E_T distribution is depicted in Fig. 2a as a function of pseudo-rapidity η. UrQMD predicts a maximum E_T of 600 GeV (with rescattering, full symbols) and a gaussian shape of the E_T distribution. Deactivating the secondary interactions (open symbols) results in a decreased energy deposition by 30% and in a plateau in the transverse energy distribution, as expected from string dynamics.

The charged particle ($\pi^+ + \pi^- + K^+ + K^-$) yields with (full symbols) and without (open symbols) rescattering are depicted in Fig. 2b.

Fig. 2c shows the E_T per charged particle as a function of pseudo-rapidity. At the central region the calculation with rescattering (full symbols) and without rescattering (open symbols) coincide. The transverse energy per particle is 600-800 MeV. However, at larger rapidities we observe secondary maxima in the calculation without rescattering - as shown below, they are due to concave momentum distributions of hadrons over rapidity.

Diquark dynamics becomes the major mechanism for the initial built-up of energy-density

[31] and particle production. It is therefore interesting to study the stopping behaviour of the present model. It has been claimed recently, that exotic mechanisms (e.g. baryon junctions [32]) need to be invoked to understand the baryon number transport at SPS and RHIC. In contrast to these approaches, the UrQMD model mainly applies quark model cross sections to the subsequent scattering of constituent (di-)quarks in combination with a small diquark breaking [33] component ($\sim 10\%$).

Figure 3a shows the rapidity spectra of protons (circles) and anti-protons (triangles) in central (b<3 fm) Au+Au reactions at $\sqrt{s} = 200$ AGeV. Full symbols denote calculations with full rescattering, whereas open symbols denote calculations without meson-meson and meson-baryon interactions. The proton distribution (in the calculation with rescattering) shows a plateau over rapidity with 20 protons at central rapidities. Without rescattering the proton distribution exhibits a dip at central rapidity values. The anti-proton distribution is of Gaussian shape with a peak value of 8 at midrapidity. It is interesting to note that the shape of the anti-proton distribution and their absolute yield stays apparently unaffected by secondary interactions. Since the overall particle production is strongly enhanced by rescattering effects (as shown below), this points to a counter balance of production and annihilation of anti-baryons.

The stopping power obtained in the full UrQMD approach is rather strong (cf. Fig. 3b). We observe a flat net-baryon rapidity distribution, while whithout rescattering two maxima develop near target/projectile rapidities and a strong dip at central rapidities. The net-proton distribution (full symbols) is shifted by approximately two units in rapidity, resulting in 12 net-protons at midrapidity. Secondary scatterings are important for transporting baryon number from projectile and target rapidity closer to midrapidity.

Figure 3c depicts the yields of negatively charged pions (neutral and positively charged pions are - on a 5% level - identical in shape and number) with full rescattering (full symbols) and without meson-meson and meson-baryon interactions (open symbols) in Au+Au, $\sqrt{s} =$ 200 AGeV, b<3 fm. Comparing the simulations with and without rescattering, a strong increase of particle production in the central rapidity region is observed if rescattering is

included. As a result, a Gaussian shape of the pions rapidity distribution emerges.

The kaon distribution is affected by secondary interactions as well, as is shown in Fig. 3d. The rapidity distributions of K^+ (circles) and K^- (triangles) with full rescattering (full symbols) and without secondary interactions (open symbols) are shown for Au+Au, $\sqrt{s} = 200$ AGeV, b<3 fm reactions. The overall amount of charged kaons increases by nearly 30% due to rescattering effects. However, the splitting between positively and negatively charged kaons seems to be unaffected by meson-meson and meson-baryon interactions. If this is the case in collisions, a possible equilibration of strangeness due to a QGP (as proposed by [38]) will not be washed out in the rescattering process and might be observable.

The charged particle abundancies, ≈ 880 at midrapidity, are in the middle of the expected multiplicity at $y = 0$ which reaches from 600 to 1200 [34,35]. It is interesting to note that the total particle yield is similar to the RQMD results [36] and also similar to a corrected pQCD based parton cascade model [27]. However, note the qualitative difference between the present results and those of a pQCD based transport approach [37]: the UrQMD calculations indicate a net-proton density of approx. 12 around midrapidity, whereas the pQCD based approach predicts a net-proton density of only 3. This large difference should allow experiments to discriminate those models.

Let us now turn to the transverse expansion dynamics: since the early UrQMD dynamics is based on string degrees of freedom, newly created quarks are not allowed to interact until they have finished their coalescence into hadrons (typically this requires 1fm/c in the local restframe of the coalescing quarks). Due to the large Lorentz γ-factor, this leads to a relatively small pressure in the initial reaction phase as compared to an equation of state which includes a phase transition to a thermalized QGP.

This behaviour is clearly visible in Fig. 4: the transverse mass distribution of protons (circles) and pions (triangles) at midrapidity ($|y| < 0.5$) are depicted for Au+Au, $\sqrt{s} =$ 200 AGeV, b<3 fm reactions. Full symbols denote calculations with full rescattering and open symbols denote calculations without secondary interactions. Without rescattering the inverse slopes of pions (open triangles) and protons (open circles) are similar. With full

rescattering (full symbols) one observes a splitting in the inverse slopes of pions and protons. Hence, secondary scatterings clearly create additional transverse flow. Note that this effect is not visible in the pion spectrum: The pion slope differences with and without rescattering are marginal. The total number of pions is decreased without rescattering.

This observation is supported by the mean transverse momenta of protons, kaons and pions, which are shown in Fig. 5 as a function of rapidity. Full lines denote calculations with full rescattering, whereas dotted lines denote calculations without rescattering. Without secondary interactions protons and pions show mean transverse momenta at central rapidities similar to the values observed in pp collisions. However, the mean transverse momenta rise strongly towards the target and projectile region. This effect is known from pp collisions as the 'sea-gull' effect [1] [39]. Frequent rescattering leads to a hydrodynamic type behaviour - this is demonstrated in Figs. 4 and 5. The mean p_T differences between proton and kaon become much larger than the difference between pion and kaon, a characteristic sign of hydrodynamic flow[2].

With full rescattering the mean transverse momenta of protons increase at central rapidities and decrease in the target/projectile region. This leads to a flat mean $p_\perp$ over rapidity. The same effect works for the kaons. In contrast, pions cool down due to rescattering (compare the dotted and full lines for pions). The cool off of pions is due to: (i) s-channel $\pi + p$ interactions which result in a splitting of pions and proton slopes due to the decay kinematics of the baryon resonances; (ii) inelastic interactions of pions lead to a destruction of the pions with high transverse momenta (high energy), e.g. $\pi + \pi \rightarrow K\overline{K}$; (ii) it is in general difficult to heat pions up to more than 140 MeV, because of production

[1]This 'sea-gull'-feature can be seen, if one plots the Feynman x_F distribution instead of the rapidity distribution.

[2]Protons always show some flow, due to the Baryon-Baryon interactions. If the model is run in pure first collision mode, this difference vanishes.

of new pions above this temperature. Pions lose part of their kinetic energy to create new hadrons and by pushing the surrounding baryons, kaons, etc. aside. Thus, the pions act as an energy reservoir for the heavier hadrons (pion wind [40]).

In conclusion, the UrQMD model has been applied to Au+Au reactions at RHIC energies. This model treats the dynamics of the hot and dense system by constituent (di-)quark and hadronic degrees of freedom. The collision spectra have been studied and the effects of secondary interactions have been quantified. Substantial baryon stopping power has been predicted. The resulting particle production has been analyzed. Secondary interactions are found to be very important for such a strong baryon stopping. They constitute a sizable source for particle production. The study of the transverse expansion of the system revealed that it is driven by pions ("pion wind"): Pions transfer their energy in the expansion phase to the heavier hadrons. As a result the pions are cooled as rescattering is included. The overall particle production is found to be similar to pQCD motivated models. However, the net-proton rapidity density at $y_{c.m.}$ differs by a factor of 4 between both approaches. This may be used to experimentally distinguish between these models.

ACKNOWLEDGEMENTS

This research used resources of the National Energy Research Scientific Computing Center (NERSC). This work is supported by the U.S. Department of Energy under contract No. DE-AC03-76SF00098, the BMBF, GSI, DFG and Graduiertenkolleg 'Theoretische und experimentelle Schwerionenphysik'. S.A. Bass is also partially supported by the DOE grant DE-FG02-96ER40945. M. Bleicher wants to thank the Nuclear Theory Group at LBNL for support and fruitful discussions.

REFERENCES

[1] S.A. Bass, M. Gyulassy, H. Stöcker and W. Greiner, J. Phys. **G25** (1999) R1.

[2] J. W. Harris, B. Müller, Ann. Rev. Nucl. Part. Sci. 46 (1996) 71

[3] J.D. Bjorken, Phys. Rev. **D27** (1983) 140.
K. Kajantie and L. McLerran, Nucl. Phys. **B214** (1983) 261.
K.J. Eskola and M. Gyulassy, Phys. Rev. **C47** (1993) 2329.

[4] R. B. Clare and D. Strottman, Phys. Reports **141** (1986) 179.
N. S. Amelin, L. P. Csernai, E. F. Staubo and D. Strottman, Nucl. Phys. **A544** (1992) 463c.
L.P. Csernai, J.I. Kapusta, G. Kluge and E.E. Zabrodin, Z. Phys. **C58** (1993) 453.

[5] D.H. Rischke and M. Gyulassy, Nucl. Phys. **A597** (1996) 701, and **A608** (1996) 479.
S. Bernard, D.H. Rischke, J.A. Maruhn, W. Greiner, Nucl. Phys. **A625** (1997) 473.

[6] A. Dumitru, D. Rischke, Phys. Rev. C 59 (1999) 354.

[7] C.M. Hung and E. Shuryak, Phys. Rev. **C57** (1998) 1891.

[8] K. Geiger, Phys. Rev. **D46** (1992) 4965 and Phys. Rev. **D46** (1992) 4986.
K. Geiger, Phys. Rev. **D47** (1993) 133.
K. Geiger, Phys. Rept. 258 (1995) 237.

[9] X. N. Wang, Phys. Rev. **D46** (1992) 1900.
X. N. Wang, Phys. Rep. 280 (1997) 287.

[10] T. Schönfeld, H. Stöcker, W. Greiner, H. Sorge, Mod. Phys. Lett. **A8** (1993) 2631,
H. Stöcker, M. Hofmann, R. Mattiello, N.S. Amelin, A. Dumitru, A. Jahns, A. von Keitz, Y. Puersuen, T. Schönfeld, C. Spieles, L.A. Winckelmann, J.A. Maruhn, W. Greiner, M. Berenguer, H. Sorge, Nucl. Phys. **A566** (1994) 15c.

[11] B. Monreal *et al.*, Phys. Rev. **C60** (1999) 031901

[12] M. Bleicher, E. Zabrodin, C. Spieles, S.A. Bass, C. Ernst, S. Soff, L. Bravina, M. Belkacem, H. Weber, H. Stöcker, W. Greiner, J. Phys. G 25 (1999) 1859;
S.A. Bass, M. Belkacem, M. Bleicher, M. Brandstetter, L. Bravina, C. Ernst, L. Gerland, M. Hofmann, S. Hofmann, J. Konopka, G. Mao, L. Neise, S. Soff, C. Spieles, H. Weber, L.A. Winckelmann, H. Stöcker, W. Greiner, C. Hartnack, J. Aichelin, N. Amelin, Progr. Nucl. Phys. 41 (1998) 225

[13] H. Sorge, H. Stocker and W. Greiner, Annals Phys. **192** (1989) 266.;
H. Sorge, Phys. Rev. C52 (1995) 3291

[14] B. Andersson, G. Gustavson, and B. Nilsson-Almquist, Nucl. Phys. **B281**, 289 (1987).

[15] B. Andersson *et al.*, Comp. Phys. Comm. **43**, 387 (1987).

[16] T. Sjoestrand, Comp. Phys. Comm. **82**, 74 (1994).

[17] L. Gerland, L. Frankfurt, M. Strikman, H. Stöcker, and W. Greiner, Phys. Rev. Lett. **81**, 762 (1998).

[18] L.V. Bravina, M.I. Gorenstein, M. Belkacem, S.A. Bass, M. Bleicher, M. Brandstetter, M. Hofmann, S. Soff, C. Spieles, H. Weber, H. Stocker, W. Greiner, Phys. Lett. B434, 379 (1998) and Phys. Rev. C 60, 024904 (1999)

[19] S.A. Bass, M. Belkacem, M. Brandstetter, M. Bleicher, L. Gerland, J. Konopka, L. Neise, C. Spieles, S. Soff, H. Weber, H. Stöcker, W. Greiner, Phys. Rev. Lett. **81** (1998) 4092;
M. Bleicher, C. Spieles, C. Ernst, L. Gerland, S. Soff, H. Stöcker, W. Greiner, S.A. Bass, Phys. Lett. B 447 (1999) 227

[20] S. Soff, S.A. Bass, M. Bleicher, L. Bravina, E. Zabrodin, H. Stöcker, W. Greiner, nucl-th/9907026, Phys. Lett. B in print

[21] C. Spieles, L. Gerland, M. Bleicher, S.A. Bass, W. Greiner, C. Lourenco, R. Vogt, Eur.

Phys. J. C 5 (1998) 349;
C. Ernst, S.A. Bass, S. Soff, H. Stöcker and W. Greiner, nucl-th/9907118.

[22] C. Spieles, R. Vogt, L. Gerland, S.A. Bass, M. Bleicher, H. Stöcker, W. Greiner, Phys. Rev. C 60 (1999) 054901

[23] M. Bleicher, M. Belkacem, C. Ernst, H. Weber, L. Gerland, C. Spieles, S.A. Bass, H. Stöcker, W. Greiner, Phys. Lett. B 435 (1998) 9;
M. Bleicher, L. Gerland, C. Spieles, A. Dumitru, S. Bass, M. Belkacem, M. Brandstetter, C. Ernst, L. Neise, S. Soff, H. Weber, H. Stöcker, W. Greiner, Nucl. Phys. **A638** (1998) 391.

[24] K. Werner, Phys. Rep. 232, 87 (1993)

[25] L. McLerran and R. Venugopalan, Phys. Rev. **D49**, 2233 and 3352 (1994)

[26] K. Eskola and X.N. Wang, Phys. Rev. **D49**, 1284 (1994)

[27] S.A. Bass and B. Müller, nucl-th/9908014.

[28] R.J. Fries, B. Müller, A. Schäfer and E. Stein, hep-ph/9907567.

[29] B. Müller, nucl-th/9906029, v3. QM '99 proceedings.

[30] H. Sorge, nucl-th/9906051, v2. QM '99 proceedings.

[31] H. Weber *et al.*, Phys. Lett. **B442**, 443 (1998)

[32] S.E. Vance, M. Gyulassy, X.N. Wang, Nucl. Phys. A 638 (1998) 395c.
D. Kharzeev, Phys. Lett. B 378 (1996) 238.

[33] A. Capella, B.Z. Kopeliovich, Phys. Lett. B 381 (1996) 325.

[34] X. N. Wang, Quark Matter '99, Turin, Italy, http://www.qm99.to.infn.it/rhic_pred/wang/wang.html

[35] S.A. Bass *et al.*, Proceedings of the RHIC-predictions session at Quark Matter '99,

nucl-th/9907090.

[36] H. Sorge, Quark Matter '99, Turin, Italy, http://www.qm99.to.infn.it/rhic_pred/sorge2/sorge.html

[37] S.A. Bass, M. Hofmann, M. Bleicher, L. Bravina, E. Zabrodin, H. Stöcker and W. Greiner, Phys. Rev.**C60** (1999) 021901.

[38] J. Rafelski, Phys. Rep. 88 (1982) 331

[39] T. Kafka et al., Phys. Rev. D16 (1977) 1261;
F. Sikler et al. (NA49 Collab.) at Quark Matter '99 Conference

[40] Y. Pang, M. Gyulassy et al., http://rhic.phys.columbia.edu/oscar

TABLES

Reaction	with rescattering	without rescattering
Baryon–Baryon	yes	yes
Baryon–Diquark	yes	yes
Baryon–Quark	yes	no
Meson–Baryon	yes	no
Meson–Diquark	yes	no
Meson–Quark	yes	no
Meson–Meson	yes	no
Diquark–Diquark	yes	yes
Quark–Diquark	yes	no
Quark-Quark	yes	no
Anti-Baryon–Baryon	yes	yes
Anti-Diquark–Diquark	yes	yes
Quark–Anti-Diquark	yes	no
Anti-Quark-Anti-Quark	yes	no

TABLE I. Possible Reaction channels with and without rescattering. Quark and Diquark refer to constituent Quarks and Diquarks at the string end points. If not especially mentioned, antiparticle reactions behave like particle reactions.

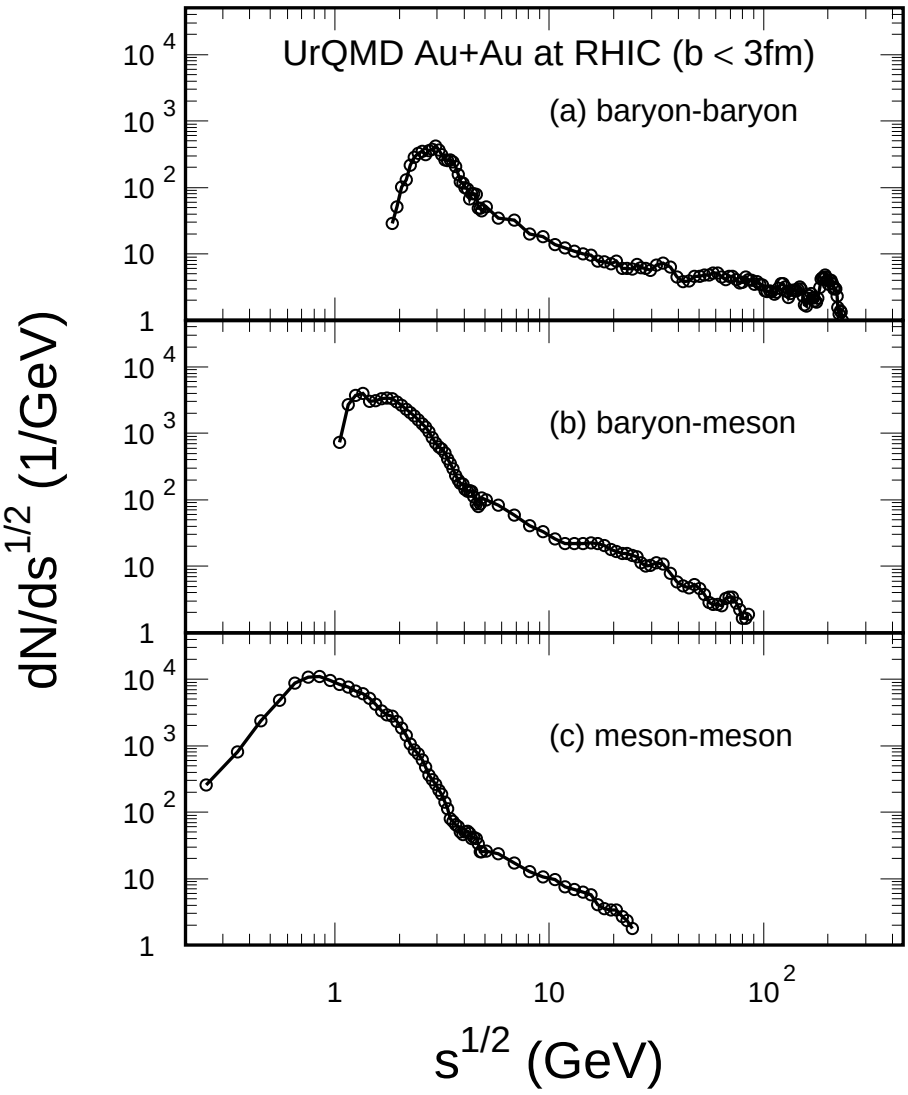

FIG. 1. Collision energy spectra of baryon-baryon (a), meson-baryon (b) and meson-meson (c) reactions in Au+Au, $\sqrt{s} = 200$ AGeV, b<3 fm.

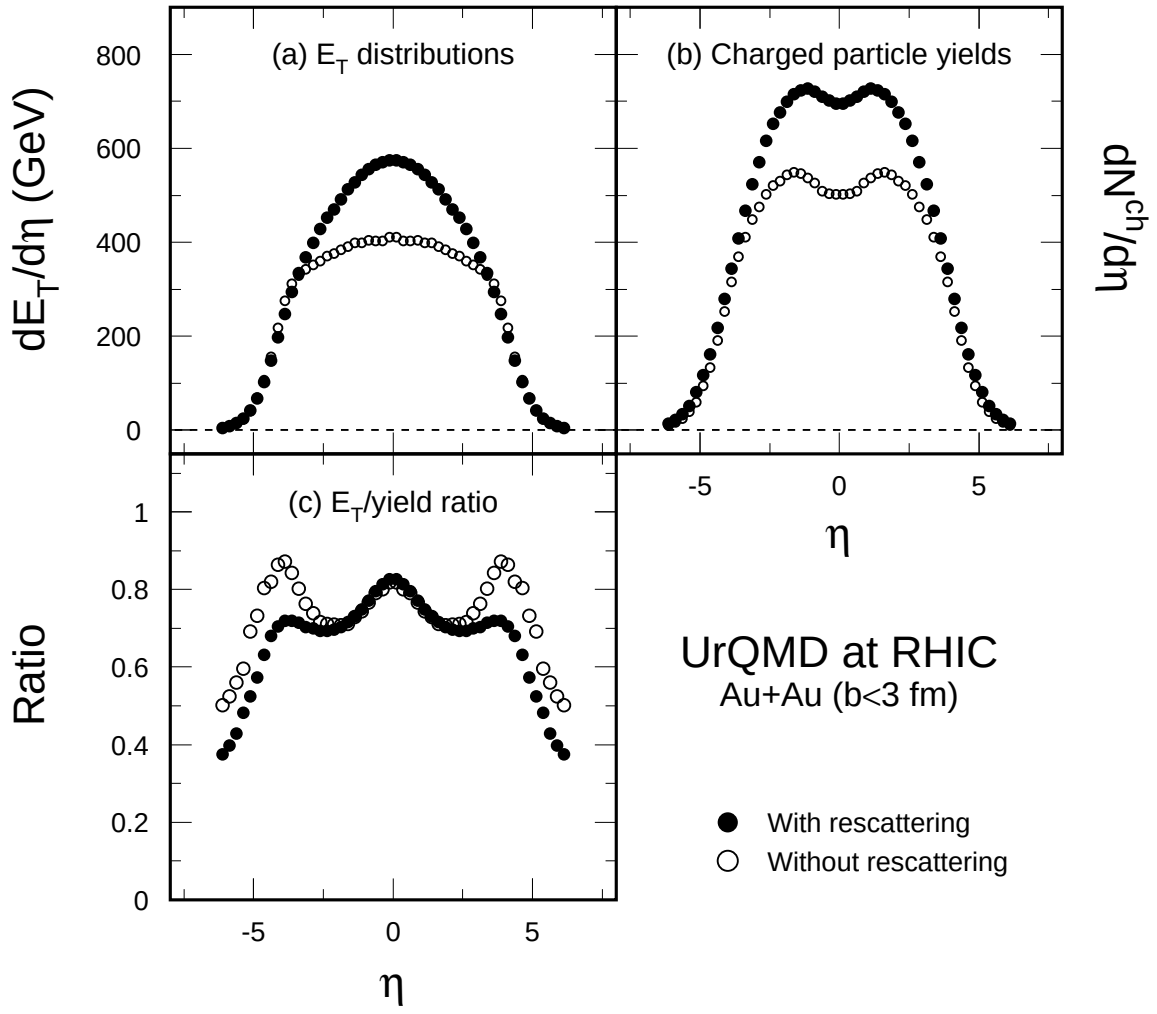

FIG. 2. Au+Au, $\sqrt{s} = 200$ AGeV, b<3 fm. Full symbols denote calculations with full rescattering. Open symbols denote calculations without meson-meson and meson-baryon interactions.

(a) Transverse energy distribution as a function of pseudo rapidity.

(b) Pseudo rapidity density of charged particles ($\pi^+ + \pi^- + K^+ + K^-$).

(c) Transverse energy per charged particle as a function of pseudo rapidity.

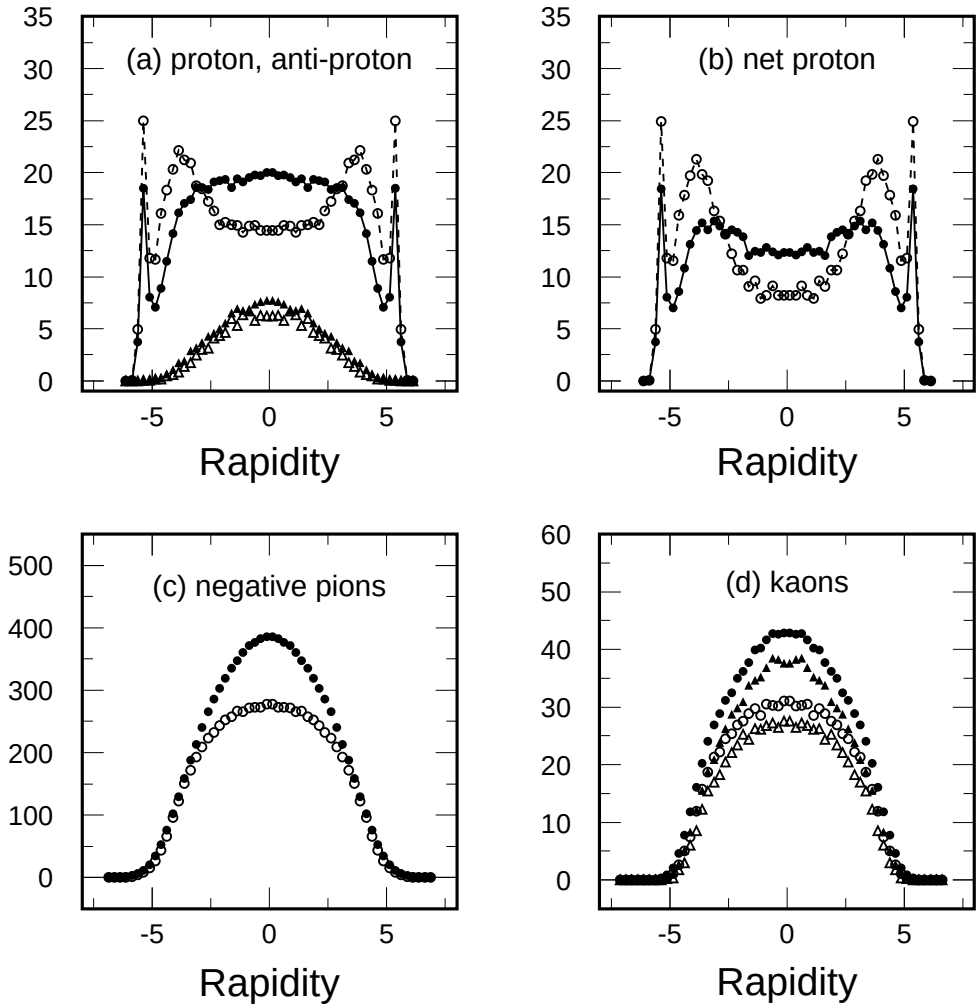

FIG. 3. Au+Au, $\sqrt{s} = 200$ AGeV, b<3 fm. Full symbols denote calculations with full rescattering. Open symbols denote calculations without meson-meson and meson-baryon interactions.

(a) Rapidity density of protons (circles) and anti-protons (triangles).

(b) Rapidity density of net-protons.

(c) Rapidity density of negatively charged pions.

(d) Rapidity density of K^+ (circles) and K^- (triangles).

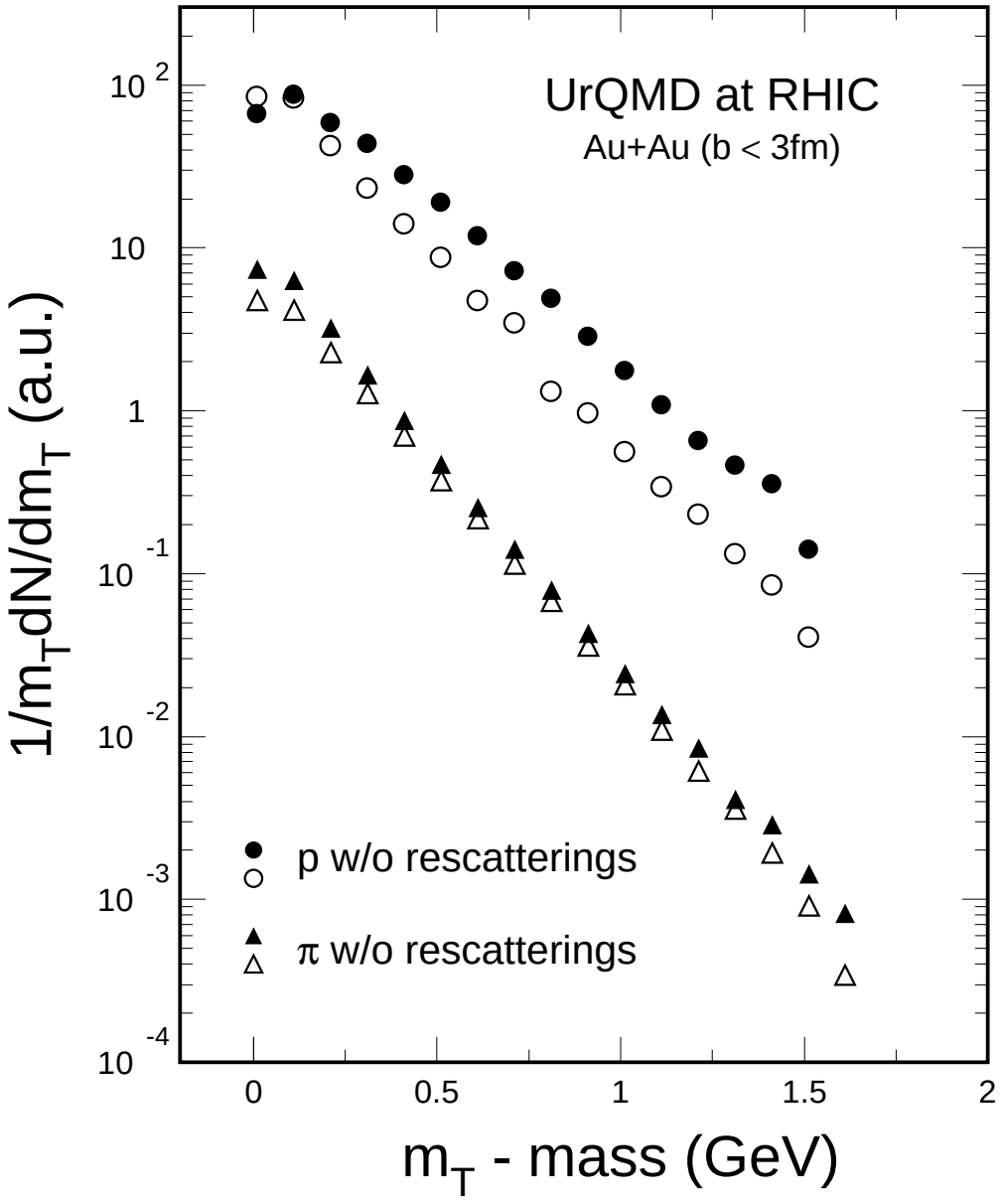

FIG. 4. Transverse mass distribution of protons (circles) and pions (triangles) at midrapidity ($|y| < 0.5$) in Au+Au, $\sqrt{s} = 200$ AGeV, b<3 fm. Full symbols denote calculations with full rescattering. Open symbols denote calculations without meson-meson and meson-baryon interactions.

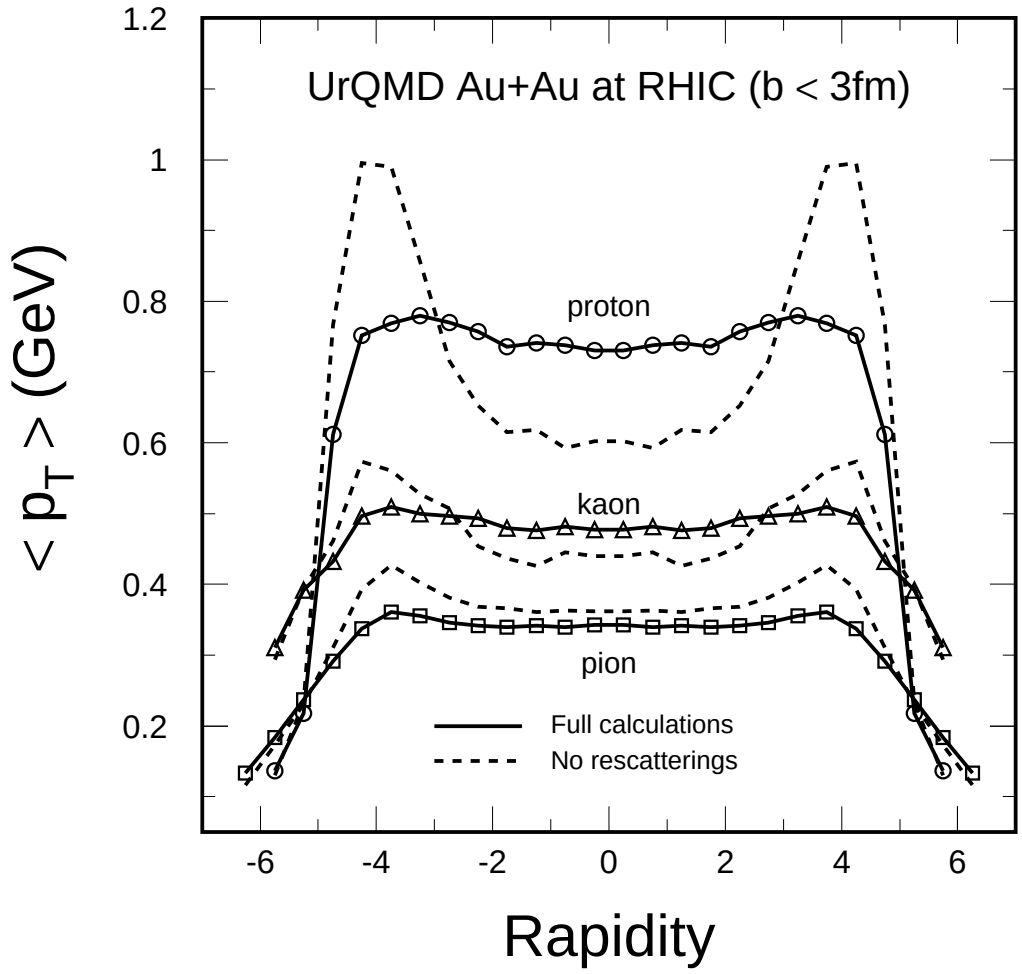

FIG. 5. Mean transverse momenta of protons, kaons and pions as a function of rapidity in Au+Au, $\sqrt{s}$ = 200 AGeV, b<3 fm. Full lines denote calculations with full rescattering. Dotted lines denote calculations without meson-meson and meson-baryon interactions.